Received: 24 October 2023 | Accepted: 8 April 2024

DOI: 10.1002/prp2.1201

ORIGINAL ARTICLE

Palliative effects of carnosol on lung-deposited pollutant particles-induced thrombogenicity and vascular injury in mice

Sumaya Beegam | Nur Elena Zaaba | Ozaz Elzaki | Abdulrahman Alzaabi | Abdulrahman Alkaabi | Khalifa Alseiari | Nasser Alshamsi | Abderrahim Nemmar

Department of Physiology, College of Medicine and Health Sciences, United Arab Emirates University, Al Ain, UAE

Correspondence
Abderrahim Nemmar, Department of Physiology, College of Medicine and Health Sciences, United Arab Emirates University, P.O. Box 15551, Al Ain, UAE.
Email: anemmar@uaeu.ac.ae; anemmar@hotmail.com

Funding information
United Arab Emirates University, Summer Undergraduate Research Experience (SURE) grant, Grant/Award Number: 2748; United Arab Emirates University, Zayed Center for Health Sciences, Grant/Award Number: 12R166; College of Medicine and Health Sciences, United Arab Emirates University, Grant/Award Number: 12M022

Abstract

The toxicity of inhaled particulate air pollution perseveres even at lower concentrations than those of the existing air quality limit. Therefore, the identification of safe and effective measures against pollutant particles-induced vascular toxicity is warranted. Carnosol is a bioactive phenolic diterpene found in rosemary herb, with anti-inflammatory and antioxidant actions. However, its possible protective effect on the thrombotic and vascular injury induced by diesel exhaust particles (DEP) has not been studied before. We assessed here the potential alleviating effect of carnosol (20 mg/kg) administered intraperitoneally 1 h before intratracheal (i.t.) instillation of DEP (20 μg/mouse). Twenty-four hours after the administration of DEP, various parameters were assessed. Carnosol administration prevented the increase in the plasma concentrations of C-reactive protein, fibrinogen, and tissue factor induced by DEP exposure. Carnosol inhibited DEP-induced prothrombotic effects in pial microvessels in vivo and platelet aggregation in vitro. The shortening of activated partial thromboplastin time and prothrombin time induced by DEP was abated by carnosol administration. Carnosol inhibited the increase in pro-inflammatory cytokines (interleukin-6 and tumor necrosis factor α) and adhesion molecules (intercellular adhesion molecule-1, vascular cell adhesion molecule-1, E-selectin, and P-selectin) in aortic tissue. Moreover, it averted the effects of DEP-induced increase of thiobarbituric acid reactive substances, depletion of antioxidants and DNA damage in the aortic tissue. Likewise, carnosol prevented the decrease in the expression of nuclear factor erythroid 2-related factor 2 (Nrf2) and heme oxygenase-1 (HO-1) caused by DEP. We conclude that carnosol alleviates DEP-induced thrombogenicity and vascular inflammation, oxidative damage, and DNA injury through Nrf2 and HO-1 activation.

Abbreviations: aPTT, activated partial thromboplastin time; CRP, C-reactive protein; DEP, diesel exhaust particles; DMSO, dimethyl sulfoxide; DNA, deoxyribonucleic acid; EDTA, ethylenediaminetetraacetic acid.; GSH, glutathione; HO-1, heme oxygenase-1; I.t., intratracheal; ICAM-1, intercellular adhesion molecule-1; IL-6, interleukin 6; TBARS, thiobarbituric acid reactive substances; KCl, potassium chloride; MDA, malondialdehyde; NaCl, sodium chloride; NBT, nitro blue tetrazolium; Nrf2, nuclear factor erythroid-derived 2-like 2; PM_{10}, particulate matter ≤10 μm; $PM_{2.5}$, particulate matter ≤2.5 μm; PT, prothrombin time; SOD, superoxide dismutase; TNFα, tumor necrosis factor α; VCAM-1, vascular cell adhesion molecule 1.

KEYWORDS
aorta, Carnosol, DNA damage, oxidative damage, particulate air pollution, thrombosis

1 | INTRODUCTION

Exposure to outdoor air pollution significantly elevates both morbidity and mortality rates, making a substantial contribution to the global burden of diseases.[1] Indeed, ambient air pollution leads to millions of premature deaths annually.[2,3] The impact of inhaling particulate matter ≤2.5 μm ($PM_{2.5}$) and the ultrafine, nanosized fraction (<0.1 μm) extends beyond the respiratory system, affecting various extrapulmonary organs. This is particularly pronounced in relation to the cardiovascular system, including the blood vessels and heart. Three primary pathophysiological pathways have been proposed to explain this phenomenon, including pulmonary inflammation triggered by inhaled particles, resulting in the release of prooxidants and inflammatory cytokines from the lungs into the bloodstream, the activation of sensory nerves by inhaled particles, and the direct passage of the nanosized fraction of particles across the alveolar-capillary barrier into the bloodstream.[2–4]

Extensive human and animal studies have established numerous pathophysiological pathways involved in the toxicity of inhaled particulate air pollution, including inflammation, oxidative damage, DNA injury, and apoptosis.[2–5] Diesel exhaust particles (DEP), a major component of urban air pollution and a source of nanoparticles, induce oxidative damage and provoke pro-inflammatory responses in vascular endothelial cells, leading to endothelial dysfunction and subsequent cardiovascular complications such as myocardial infarction, ischemia, and prothrombotic events.[2,5] Beyond reducing air pollution levels, the utilization of efficient and cost-effective pharmacological agents with anti-inflammatory and antioxidant properties could be beneficial in preventing or mitigating the effects of inhaled particulate air pollution, particularly in individuals vulnerable to air pollution and those unavoidably exposed to high levels of air pollution.[2]

Carnosol is a phenolic diterpenoid found in the extract of rosemary (*Rosmarinus officinalis*) and possesses a range of pharmacological properties, including antioxidant, anti-inflammatory, anti-cancer, and anti-microbial actions.[6–8] Previous studies have demonstrated that carnosol can modulate several signaling pathways associated with the progression of inflammatory and oxidative stress-related disorders, including asthma, liver injury, colitis, and arthritis.[6,7,9] However, to the best of our knowledge, no study has investigated the potential protective effects of carnosol against the thrombogenicity and vascular injury induced by a relevant type of pollutant particles, specifically DEP.

Therefore, the primary objective of this study was to assess the potential ameliorative effects of carnosol on the adverse impacts of pulmonary DEP deposition on the blood and vasculature of mice. These assessments encompassed platelet aggregation both in vivo and in vitro, vascular inflammation, oxidative damage, DNA injury, as well as the expression of nuclear factor erythroid-derived 2-like 2 (Nrf2) and heme oxygenase-1 (HO-1).

2 | MATERIALS AND METHODS

2.1 | DEP and carnosol

The DEP were acquired from the National Institute of Standards and Technology (located in Gaithersburg, MD, USA) and were subsequently suspended in sterile saline (0.9%) containing 0.01% Tween 80. Before dilution and intratracheal (i.t.) administration of the DEP, the suspensions were subjected to continuous sonication (using a Clifton Ultrasonic Bath, Clifton, NJ, USA) for a duration of 15 min, followed by vortexing. Control mice received i.t. instillation of saline containing 0.01% Tween 80. A prior examination using transmission electron microscopy of the DEP utilized in this research unveiled the presence of various small aggregates of carbonaceous particles of less than 0.1 μm, as well as larger aggregates with diameters less than 1 μm.[10] The chemical examination of these DEP revealed the existence of elemental carbon, organic carbon, polycyclic aromatic hydrocarbons, inorganic ions, as well as various metals and trace elements through chemical analysis.[11] Carnosol was procured from Sigma Chemical, located in St. Louis, MO, USA.

2.2 | Animals and treatments

A total number of 84 BALB/C mice (UAEU, College of Medicine and Health Sciences, animal house) were used in this study. The latter included the mice used for the assessments of biochemical parameters measured [32 mice ($n = 8 \times 4$ groups)], thrombosis [32 mice ($n = 8 \times 4$ groups)] and DNA damage assessed by Comet assay [20 mice ($n = 5 \times 4$ groups)]. BALB/C mice, approximately 8 weeks old and weighing around 20 g, were housed in rooms with a 12-h light and 12-h dark cycle at a temperature of 22 ± 1°C. They had unrestricted access to tap water and commercially available chow.

To introduce the DEP into the lungs, we employed i.t. instillation technique.[12,13] The mice were initially anesthetized using 5% isoflurane delivered via a Surgivet® model 100 vaporizer. They were then placed in a supine position with their necks extended on an angled board. A 24 Gauge Becton Dickinson cannula was carefully inserted through the mouth into the trachea. Subsequently, either a suspension of DEP at a dose of 20 μg per mouse or a saline solution (0.9% NaCl containing 0.01% Tween 80) was instilled into the trachea in a volume of 100 μL using a sterile syringe, immediately followed by a 100 μL air bolus.

Carnosol was administered through intraperitoneal injection (20 mg/kg) 1 h before the i.t. instillation of either DEP or saline. This particular dose of carnosol was selected based on previous studies demonstrating its safety and efficacy in various animal models, including those of unilateral ureteral obstruction, spinal cord injury, experimental autoimmune encephalomyelitis, and fibrosarcoma.[7,14,15]

The mice were divided into four equal groups and treated as follows:

- Group 1: Received normal saline via intraperitoneal injection 1 h before i.t. instillation of saline.
- Group 2: Received normal saline via intraperitoneal injection 1 h before i.t. instillation of DEP (20 μg/mouse).
- Group 3: Received carnosol (20 mg/kg) via intraperitoneal injection 1 h before i.t. instillation of saline.
- Group 4: Received carnosol (20 mg/kg) via intraperitoneal injection 1 h before i.t. instillation of DEP (20 μg/mouse).

Twenty-four hours after the deposition of DEP or saline into the lungs, we assessed several parameters.

2.2.1 | Experimental microvessel thrombosis model

The assessment of thrombogenicity in mice treated with either DEP or saline, with or without carnosol administration, was conducted in pial arterioles and venules using a previously described technique.[16–18] In brief, the experimental procedure involved the administration of urethane anesthesia (1 mg/g body weight, intraperitoneal) to the animal. Subsequently, tracheal intubation was performed, and a 2F venous catheter (Portex, Hythe, UK) was inserted into the right jugular vein for the infusion of fluorescein (Sigma-Aldrich, St. Louis, MO, USA). A craniotomy was then conducted on the right temporoparietal cortex using a hand-held microdrill, with careful removal of the dura. Only preparations without any trauma to microvessels or underlying brain tissue were utilized, discarding any showing signs of damage. The direct visualization of cerebral microcirculation was achieved through a fluorescence microscope (Olympus, Melville, NY, USA) connected to a camera and DVD recorder. The animal's body temperature was maintained at 37°C using a heating pad, monitored by a rectal thermoprobe connected to a temperature reader (Physitemp Instruments, NJ, USA). A specific field containing arterioles and venules with diameters ranging from 15 to 20 μm was selected for observation. This field was recorded both before and during the photochemical insult. The photochemical insult was induced by injecting fluorescein (0.1 mL/mouse of 5% solution) via the jugular vein, allowing it to circulate for 30–40 s. Following this, the cranial preparation was exposed to stabilized mercury light. The resulting injury to arterioles and venules prompted the adherence and aggregation of platelets at the damaged endothelial sites. Over time, platelet aggregates and thrombus formation increased in size until complete vascular occlusion occurred.[16–18] The duration from the initial injury to complete vascular occlusion (time to flow stop) in arterioles and venules was measured in seconds. Upon conclusion of the experiments, the animals were euthanized using an overdose of urethane.

2.2.2 | Platelet aggregation in whole blood in vitro

Platelet aggregation in whole blood was assessed in vitro, as previously reported.[16–18] After exposure to DEP or saline, with or without carnosol injection, mice were anesthetized (via intraperitoneal injection of sodium pentobarbital at 45 mg/kg), and blood was collected from the inferior vena cava into citrate (3.8%). The blood from different mice was not pooled. Aliquots of 100 μL were added to the well of a coagulometer (MC 1 VET, Merlin, Lemgo, Germany). The blood samples were then incubated with 0.1 μM adenosine diphosphate (ADP) for 3 min and stirred for three more minutes. Subsequently, 25 μL samples were taken and fixed on ice in cellFix (225 mL) (Becton Dickinson, Franklin Lakes, NJ). Following fixation, single platelets were counted using a VET ABX Micros with a mouse card (Montpellier, France). Platelet aggregation was determined by quantifying the decrease in single platelets due to ADP (0.1 μM)-induced aggregation.[16–18]

2.2.3 | Activated partial thromboplastin time (aPTT) and prothrombin time (PT) assessment in vitro

In vitro evaluation of aPTT and PT in blood was carried out as previously described.[19,20] After pulmonary administration of DEP or saline, with or without carnosol treatment, animals were anesthetized as indicated earlier, and blood was collected from the inferior vena cava and mixed with 3.8% citrate solution (blood to anticoagulant ratio: 9:1). PT was assessed on freshly obtained platelet-poor plasma using recombiplastin (human relipidated recombinant thromboplastin) from Instrumentation Laboratory (Orangeburg, NY, USA) with a coagulometer (MC 1 VET, Merlin, Lemgo, Germany). Similarly, aPTT was determined using the automated aPTT reagent from bioMerieux (Durham, NC, USA) on the same coagulometer.

2.2.4 | Measurement of C-reactive protein (CRP), fibrinogen, and tissue factor in the plasma

After exposure to either saline or DEP, with or without carnosol injection, animals were anesthetized as previously described. Blood was collected from the inferior vena cava in 4% EDTA and centrifuged at 900 *g* for 15 min at 4°C. Plasma specimens obtained were stored at −80°C until further biochemical analysis. The blood from different mice was not pooled. The concentrations of CRP (GenWay Biotech, Inc., San Diego, CA, USA), fibrinogen (Molecular Innovation,

Southfield, MI, USA), and tissue factor (Molecular Innovation, Southfield, MI, USA) were quantified using commercially available ELISA kits.

2.2.5 | Measurement of P-selectin, E-selectin, vascular cell adhesion molecule 1 (VCAM-1), and intercellular adhesion molecule-1 (ICAM-1) in aortic homogenates

Preparation of aortic homogenates for the quantification of P-selectin, E-selectin, VCAM-1, and ICAM-1 was performed as previously described.[21] Concentrations of P-selectin, E-selectin, VCAM-1, and ICAM-1 were determined using ELISA kits purchased from R&D Systems (Minneapolis, MN, United States).

2.2.6 | Measurement of tumor necrosis factor α (TNFα), interleukin (IL)-6, thiobarbituric acid reactive substances (TBARS), superoxide dismutase (SOD), glutathione (GSH), and heme oxygenase-1 (HO-1) in aortic homogenates

TNFα and IL-6 concentrations were determined in aortic homogenates and plasma using ELISA Duo Set kits obtained from R&D Systems (Minneapolis, MN, United States).

NADPH-dependent membrane lipid peroxidation was quantified as thiobarbituric acid reactive substances with malondialdehyde (MDA) as a standard (Sigma, Saint Louis, MO, United States). MDA has been extensively utilized as an indicator of lipid peroxidation due to its easy reaction with thiobarbituric acid.[22,23] This reaction results in the formation of MDA-thiobarbituric acid, a conjugate that absorbs light in the visible spectrum at 532 nm, resulting in a red-pink color.[22,23] In addition to MDA, other molecules stemming from lipid peroxidation can also react with thiobarbituric acid, absorbing light at 532 nm. This contributes to the overall absorption signal that is quantified.[22,23] Consequently, this assay is recognized for measuring TBARS,[22–24] and it has been suggested that when employed and interpreted accurately, the TBARS assay is commonly regarded as a reliable indicator reflecting the overall extent of oxidative stress within a biological sample.[22,23]

GSH concentration was measured as protein-free sulfhydryl content by the method of Tietze as described before[25] and according to the vendor's protocol (Sigma, Saint Louis, MO, United States). The conversion of xanthine to uric acid and hydrogen peroxide by xanthine oxidase was used as the basis for the measurement of SOD. SOD inhibited the reduction of nitro blue tetrazolium (NBT) to NBT-diformazan by superoxide ions, which was linearly related to the xanthine oxidase activity. SOD activity was thus measured as the % inhibition of NBT-diformazan formation[26] following the supplier's instructions (Cayman Chemicals, MI, United States). HO-1 was quantified using a mouse ELISA Kit purchased from Abcam (Cambridge, UK).

2.2.7 | DNA damage in aortic tissue

Immediately following euthanasia, the aortas were excised from each animal.[27,28] Single-cell suspensions from the diverse hearts were obtained following established protocols.[27,28] Each harvested aorta was rinsed in a chilled medium composed of Roswell Park Memorial Institute medium-1640, 15% DMSO, and 1.8% (wt/vol) NaCl. Subsequently, the aorta was placed in 1.5 mL of the medium and finely chopped into small fragments in a petri dish using scissors. The fragments were allowed to settle, and the resulting supernatant was collected in a 15-ml tube. The obtained cell suspension underwent centrifugation at 900 g for 5 min at 4°C. The supernatant was discarded, and the pellets were resuspended in 0.5 mL of the medium. These cell suspensions were combined with a low-melting-point agarose solution (0.65%) and applied onto agarose (1.5%)-precoated microscope slides. For each treatment, five slides were prepared, and they were then incubated in ice-cold lysis buffer (2.5 M NaCl, 10 mM Tris, 100 mM EDTA, 1% Triton X-100, and 10% DMSO) at 4°C for at least 1 h to eliminate cell membranes. Following incubation, the slides were placed in a horizontal electrophoresis unit and exposed to electrophoresis buffer (0.2 M EDTA and 5 M NaCl, pH 10) for 20 min to facilitate DNA unwinding and the expression of alkali-labile sites. Electrophoresis was carried out for 20 min at 25 V and 300 mA. After electrophoresis, the slides were neutralized with Tris buffer (0.4 M Trizma base, pH 7.5) for 5 min and washed with methanol. Subsequently, the slides were stained with propidium iodide, as previously described.[27,28] All procedures were conducted in darkness to prevent additional DNA damage. The slides were mounted on a fluorescent microscope, and cell scoring was performed. Fifty cells from each treatment were scored and analyzed for DNA migration, with the average of five slides from each group calculated. The measurement of the length of DNA migration (i.e., diameter of the nucleus plus migrated DNA) was determined using image-analysis Axiovision 3.1 software (Carl Zeiss).[27,28]

2.2.8 | Western blot analysis for nuclear factor erythroid 2-related factor 2 (Nrf2) expression in the aorta

Western blotting was employed to measure the protein expression of Nrf2.[29] Aortic tissues collected from the mice were rapidly frozen with liquid nitrogen and stored at −80°C. Subsequently, the tissues were weighed, rinsed with 0.9% NaCl, and homogenized using lysis buffer (pH 7.4) comprising 140 mM NaCl, 300 mM KCl, 10 mM trizma base, 1 mM EDTA, Triton X-100 (0.5/100 mL distilled water), sodium deoxycholate (0.5 g/100 mL distilled water), and phosphatase and protease inhibitors. The aortic homogenates were centrifuged at 4°C for 20 min, and the supernatants were collected. Protein quantification was performed using a Pierce bicinchoninic acid protein assay kit (Thermo Scientific, Waltham, Massachusetts, USA). A 70 μg protein sample was separated by electrophoresis on a 10% sodium dodecyl sulfate polyacrylamide gel and transferred onto polyvinylidene difluoride membranes.

The immunoblots were blocked with 5% non-fat milk and then probed overnight at 4°C with a monoclonal rabbit Nrf2 antibody (1:2000 dilution) from Abcam (Cambridge, UK). The blots were subsequently incubated with a goat anti-rabbit IgG horseradish peroxidase-conjugated secondary antibody (1:5000 dilution, Abcam) at room temperature for 2 h and developed using the Pierce enhanced chemiluminescent and Western blotting substrate Kit (Thermo Scientific). Densitometry analysis of the protein bands was performed using Typhoon FLA 9500 (GE Healthcare Bio-Sciences, Uppsala, Sweden). The blots were then re-probed with a mouse monoclonal GAPDH antibody (1:5000 dilution) from Abcam (Cambridge, UK) and used as a control.

2.3 | Statistical analysis

Statistical analysis was conducted using version 7 of GraphPad Prism (GraphPad Software Inc, San Diego, CA, USA). Group comparisons were made using one-way analysis of variance followed by Holm–Sidak's multiple comparisons test. *p*-values less than .05 were considered statistically significant.

3 | RESULTS

3.1 | Impact of DEP on the plasma concentrations of CRP, fibrinogen and tissue factor, and the effect of carnosol thereon

I.t. instillation of DEP significantly increased CRP, fibrinogen, and tissue factor concentrations in plasma ($p < .01$) (Figure 1). Carnosol treatment prevented these increases ($p < .01$), restoring their levels to those seen in the carnosol+saline group (Figure 1).

3.2 | Influence of DEP on pial microvascular thrombosis, and the effect of carnosol thereon

DEP exposure resulted in increased thrombogenicity in pial arterioles and venules, reflected in shorter thrombotic occlusion times ($p < .0001$) (Figure 2). Carnosol+DEP group showed a significant improvement compared with the DEP-exposed group ($p < 0.0001$) (Figure 2). Thrombotic occlusion time was similar between carnosol+DEP and carnosol+saline groups in pial arterioles but showed a slight but statistically significant difference in pial venules ($p < 0.0001$) (Figure 2).

3.3 | Impact of DEP on platelet aggregation in whole blood, and the effect of carnosol thereon

DEP exposure increased platelet aggregation when incubated with ADP (0.1 μM), leading to a decrease in single platelet count ($p < .0001$) (Figure 3). Carnosol pretreatment significantly mitigated DEP-induced platelet aggregation ($p < 0.0001$) (Figure 3). A slight but statistically significant difference was observed between carnosol+DEP and carnosol+saline groups ($p < 0.01$) (Figure 3).

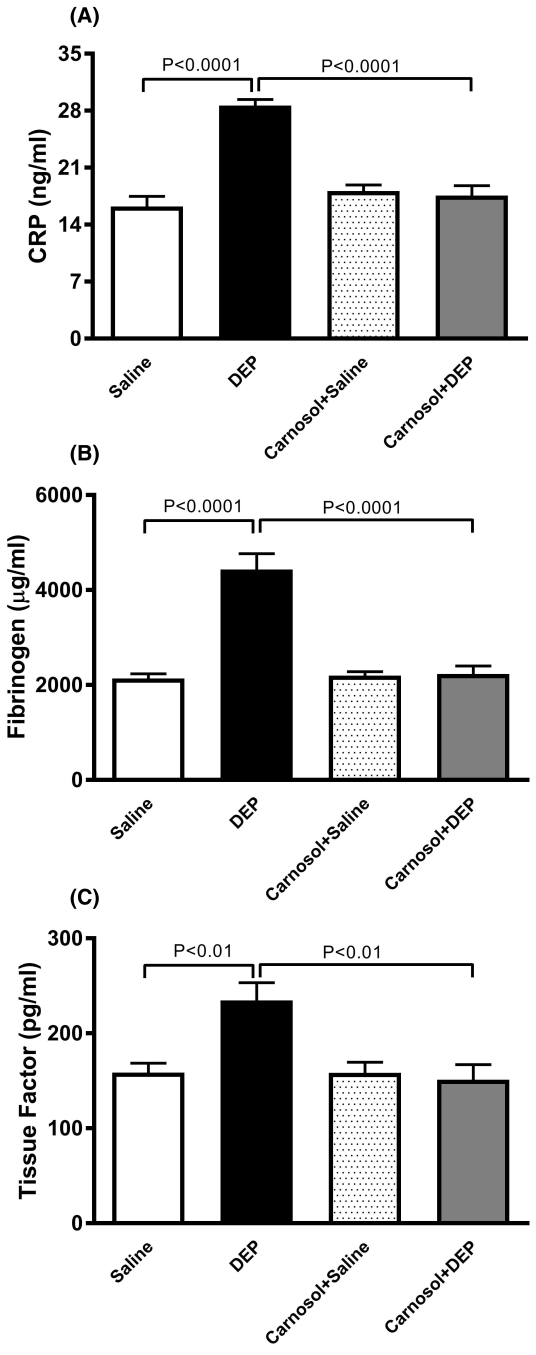

FIGURE 1 Plasma concentrations of C-reactive protein (CRP) (A), fibrinogen (B), and tissue factor (C), 24 h after pulmonary administration of either saline or diesel exhaust particles (DEP; 20 μg/mouse) with or without carnosol pretreatment (20 mg/kg) given 1 h earlier. Data are expressed as means ± SEM ($n = 8$). Statistical analysis was by Holm–Sidak's multiple comparisons test.

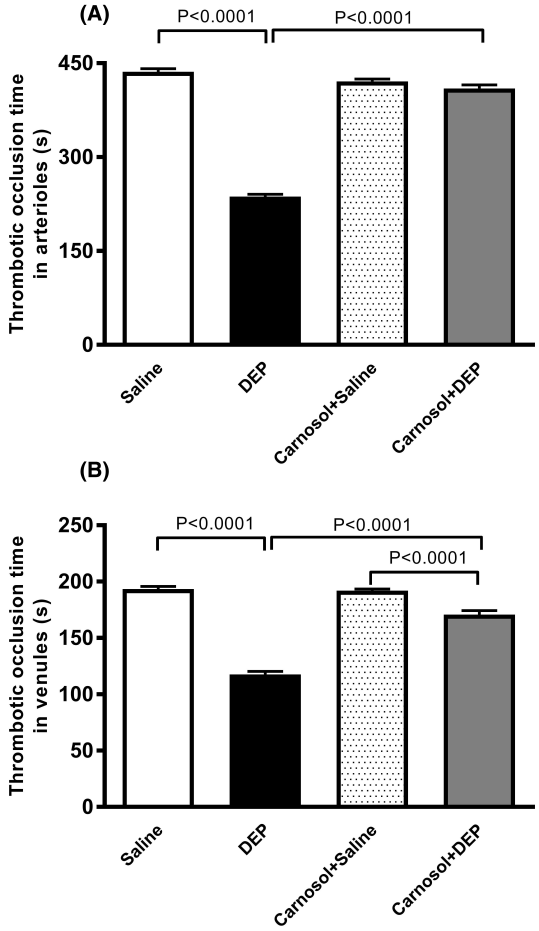

FIGURE 2 Thrombotic occlusion time in pial arterioles (A) and venules (B), 24 h after pulmonary administration of either saline or diesel exhaust particles (DEP; 20 μg/mouse) with or without carnosol pretreatment (20 mg/kg) given 1 h earlier. Data are means ± SEM ($n = 8$). Statistical analysis was by Holm–Sidak's multiple comparisons test.

3.4 | Action of DEP on PT and aPTT in vitro, and the effect of carnosol thereon

As shown in Figure 4, DEP instillation significantly shortened both PT and aPTT ($p < .0001$). Carnosol treatment prevented this effect ($p < 0.0001$), with a small but statistically significant difference in aPTT between carnosol+DEP and carnosol+saline groups ($p < 0.0001$).

3.5 | Effect of DEP on the concentrations of P-selectin, E-selectin, ICAM-1, and VCAM-1 in aortic tissue, and the influence of carnosol thereon

DEP exposure markedly increased concentrations of P-selectin, E-selectin, ICAM-1, and VCAM-1 in aortic tissue homogenates ($p < 0.0001$) (Figure 5). Carnosol treatment significantly prevented these effects ($p < 0.0001$) (Figure 5).

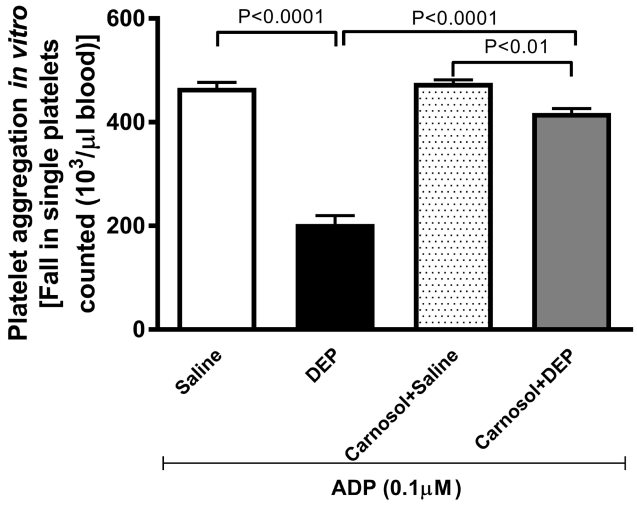

FIGURE 3 Platelet aggregation in whole blood incubated with ADP (0.1 μM). The blood was collected from mice, 24 h after pulmonary administration of either saline or diesel exhaust particles (DEP; 20 μg/mouse) with or without carnosol pretreatment (20 mg/kg) given 1 h earlier. Platelet aggregation was assessed by estimating the fall in single platelets, counted due to aggregation induced by ADP. Data are means ± SEM ($n = 8$). Statistical analysis was by Holm–Sidak's multiple comparisons test.

3.6 | Impact of DEP on the concentrations of IL-6 and TNFα in aortic tissue homogenates and plasma, and the effect of carnosol thereon

Figure 6 illustrates that DEP exposure led to a significant increase in concentrations of IL-6 and TNFα in both aortic tissue homogenates and plasma ($p < .001$). Combining carnosol with DEP administration significantly reduced IL-6 and TNFα levels compared with DEP-exposed group ($p < .05$). In aortic tissue homogenates, a statistically significant difference was observed in TNFα concentration between carnosol+DEP and carnosol+saline groups ($p < .05$).

3.7 | DEP effects on the concentrations of TBARS and GSH, and activity of SOD in aortic tissue homogenates, and the influence of carnosol thereon

Figure 7 shows that DEP exposure significantly increased TBARS concentration and decreased SOD activity and GSH concentration ($p < .0001$). Combining carnosol with DEP significantly prevented the increase in TBARS and restored SOD and GSH levels ($p < .0001$).

3.8 | Impact of DEP on the DNA damage in aortic tissue, and the effect of carnosol thereon

As displayed in Figure 8, i.t. instillation of DEP caused DNA damage ($p < .0001$). Carnosol treatment effectively prevented this effect ($p < .0001$).

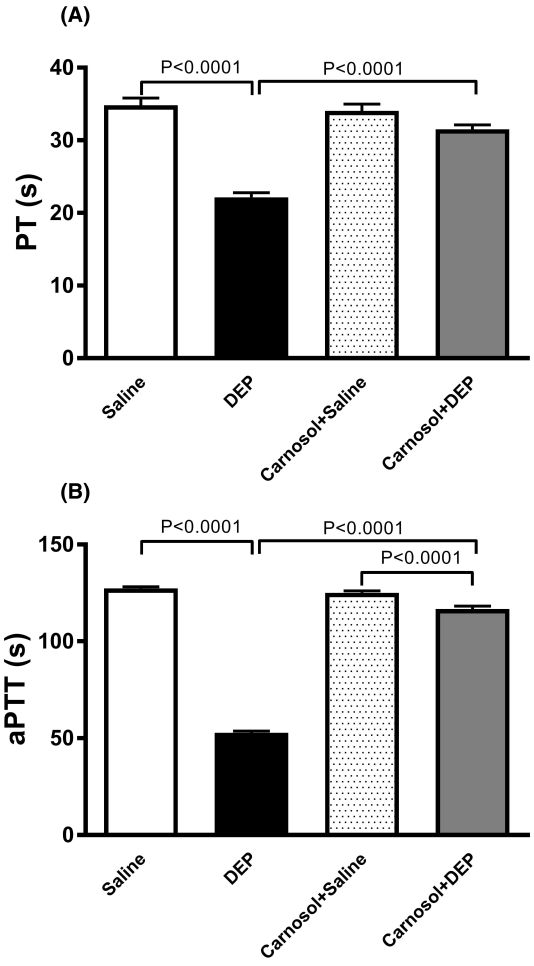

FIGURE 4 Prothrombin time (PT; A) and activated partial thromboplastin time (aPTT; B) measured on plasma samples, 24 h after pulmonary administration of either saline or diesel exhaust particles (DEP; 20 μg/mouse) with or without carnosol pretreatment (20 mg/kg) given 1 h earlier. Data are means ± SEM ($n = 8$). Statistical analysis was by Holm–Sidak's multiple comparisons test.

3.9 | Impact of DEP on the levels of Nrf2 and HO-1 in aortic tissue homogenates, and the effect of carnosol thereon

DEP exposure decreased Nrf2 expression in aortic homogenates ($p < .0001$). The latter was significantly prevented by carnosol treatment ($p < .0001$) (Figure 9A). HO-1 levels were reduced by DEP exposure, but this effect was averted by carnosol treatment ($p < .0001$) (Figure 9B).

4 | DISCUSSION

In this study, we provide robust evidence that pretreatment with carnosol exerts a significant protective effect against the prothrombotic events, vascular inflammation, oxidative damage, and DNA injury induced by DEP exposure. This beneficial impact is achieved through the activation of Nrf2 and HO-1.

It has been reported that half of the mortality related to air pollution resulted from cardiovascular diseases.[30] The latter effects are seen even at levels of $PM_{2.5}$ below the present WHO and national limits.[30] Also, and importantly over 90% of the worldwide population lives in zones where the WHO annual air quality standard for $PM_{2.5}$ is surpassed.[31] Of note, it has been reported that short-term exposure (lag 1-day exposure) to $PM_{2.5}$ was significantly linked with myocardial infarction mortality.[32] In the present study, we assessed the acute effects (24 h) of a relevant type of particulate air pollution, viz. DEP on vascular homeostasis.

The pulmonary exposure to DEP was executed by i.t. instillation which is widely used, and was reported to be a valid and accurate way of pulmonary delivery of particles.[12,13,33] The use of phytochemicals and pharmacological agents to avert or mitigate the impact of inhaled particulate air pollution possesses the advantages of clarifying mechanisms and has the potential to alleviate the toxicity of these pollutants in healthy people and those with pre-existing chronic medical conditions.[3]

In the present study, we used carnosol, a phenolic diterpenoid found in rosemary extracts, which has various anti-inflammatory, anti-tumor, and antioxidant actions.[7] To our knowledge, no clinical trial has been conducted on this compound.[2] Nonetheless, there is evidence suggesting that Mediterranean products, such as rosemary, may offer promising benefits in treating metabolic syndrome.[6] Although limited, some clinical trials have investigated the effects of rosemary extract and its polyphenols on dyslipidemia. In one study, participants were segregated into three groups and given 2, 5, or 10 g/day of dried rosemary leaf powder for 2 months.[3,4] The findings showed that rosemary treatment led to reductions in fasting plasma glucose, total cholesterol, triglycerides, and LDL-C levels, along with an increase in HDL-C levels. These effects were linked to a decrease in malondialdehyde and glutathione reductase levels, and an increase in vitamin C and β-carotene content.[3,4] Additionally, another observational study in humans demonstrated that rosemary powder (3 g/day for 4 weeks) provided protective effects on lipid profiles and blood glucose levels in both type 2 diabetic patients and nondiabetic individuals over 40 years old.[4,5] In the current study, carnosol was injected intraperitoneally. Several studies have adopted this mode of administration.[7] Intraperitoneal administration is acknowledged as a parenteral route for drug delivery. Parenteral administration methods typically offer the highest bioavailability by bypassing the common first-pass effect associated with oral administration. Consequently, when utilizing intraperitoneal administration, the dosage tends to be comparatively lower than that required for oral administration.[7,34] The dosage for intraperitoneal administration of carnosol in rodents ranged from 0.5 to 50 mg/kg,[7,14,15] and no unwanted side effects were reported. Hence, the intraperitoneal dosage used in the current study (20 mg/kg) is comparable to the aforementioned studies and did not show any side effects as none of the endpoints measured was affected by carnosol alone (no difference between the saline vs. carnosol+saline groups was seen for any of the parameter assessed). The effect carnosol on particulate air pollution-induced vascular pathophysiologic effects has not been

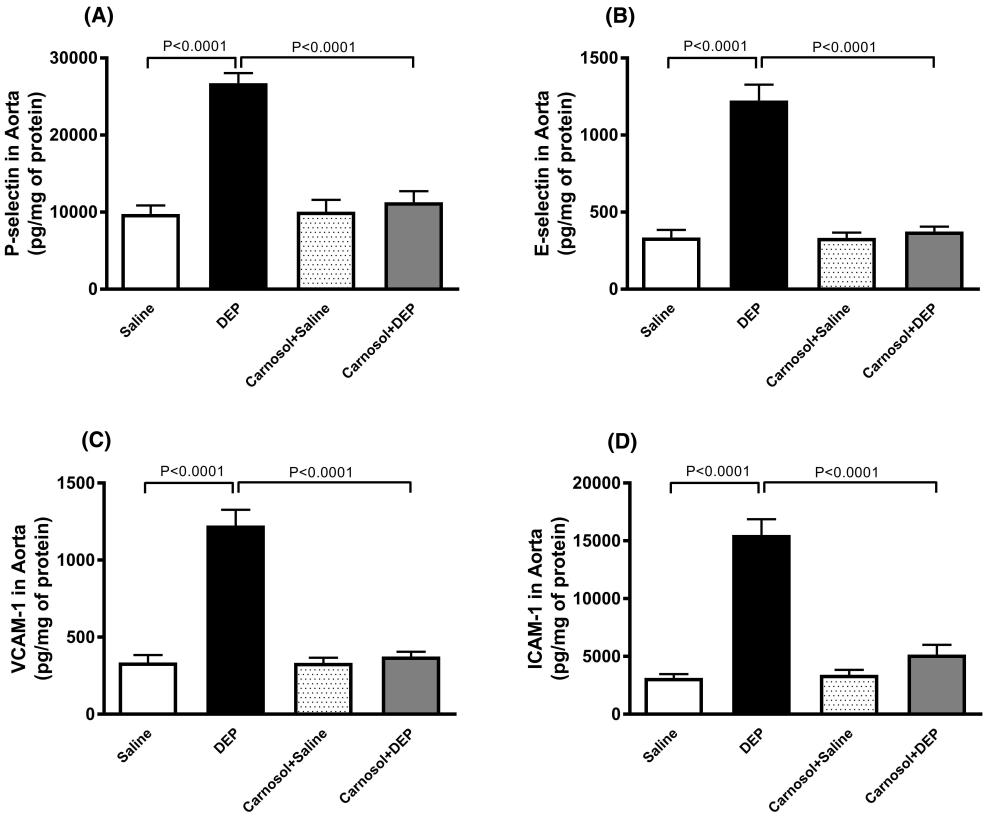

FIGURE 5 P-selectin (A), E-selectin (B), vascular cell adhesion molecule 1 (VCAM-1; C) and intercellular adhesion molecule-1 (ICAM-1; D) concentrations in aortic tissue homogenates, 24 h after pulmonary administration of either saline or diesel exhaust particles (DEP; 20 μg/mouse) with or without carnosol pretreatment (20 mg/kg) given 1 h earlier. Data are means ± SEM ($n = 8$). Statistical analysis was by Holm–Sidak's multiple comparisons test.

tested yet. Our data show that carnosol significantly prevented DEP-induced increase in CRP, fibrinogen, and tissue factor concentrations in plasma. It also averted the increased of thrombogenicity in pial arterioles and venules in vivo, and platelet aggregation in vitro. A previous study has reported that carnosol displays an effective antiplatelet activity in vitro in rabbit platelets without any cytotoxicity and that this action was mainly mediated by the inhibition of thromboxane A2 receptor and cytosolic calcium mobilization.[35] Global coagulation assays may offer a broader depiction of hemostatic status. A reduction in PT and aPTT points to a greater coagulability of the blood. It has been shown that exposure to particulate air pollution caused a significant shortening in PT and aPPT in healthy subjects following short-term exposure to particulate air pollution.[36,37] Our data confirm the shortening of PT and aPTT following DEP exposure. The observed shortening of PT is consistent with the increase in plasma concentration of tissue factor. Moreover, the elevation of fibrinogen concentration in plasma is compatible with the shortening of PT and aPTT. All the aforementioned actions were potently and significantly averted by carnosol pretreatment highlighting the potent antithrombotic effect of carnosol both in vivo and in vitro.

Vascular adhesion molecules comprising of P-selectin, E-selectin, VCAM-1, and ICAM-1 are expressed on endothelial cells and control the recruitment of white blood cells (WBCs) at various stages of inflammation.[38] It has been shown that exposure to particulate air pollution impairs vascular homeostasis, and elevates the expression of vascular inflammatory biomarkers, comprising ICAM-1 and VCAM-1, and P-selectin.[38] ICAM-1, VCAM-1 and P-selectin exert a central role in thrombogenicity through the promotion of interactions between WBCs endothelial cells and WBCs platelets in inflammatory reactions.[38] E-selectin is essential for the primary rolling interaction and ensuing adhesion of WBCs in the inflamed endothelium, in addition to the transmigration of inflammatory cells to areas of inflammation. It has reported that exposure to particulate air pollution induces the upregulation of VCAM-1, ICAM-1, P-selectin, and E-selectin.[39] Our data show that DEP induced substantial increase of P-selectin, E-selectin, VCAM-1, and ICAM-1 concentrations in the aortic homogenate and that the combination of carnosol treatment with DEP instillation has potently prevented these effects. Our results are in agreement with previous in vitro findings which reported that carnosol inhibits the expression of cell adhesion molecules and chemokines in human umbilical vein endothelial cells induced by TNF-α.[40,41]

Vascular risk factors including air pollution, trigger endothelium activation from the quiescent state to that of host defense response.[2,42] In the course of endothelial activation, that is, endothelial dysfunction, cells trigger a molecular process which initiates the generation of pro-inflammatory cytokines and oxidant instigating inflammation, oxidative damage, cytotoxicity, and genotoxicity.[2,42] Here, in order to assess

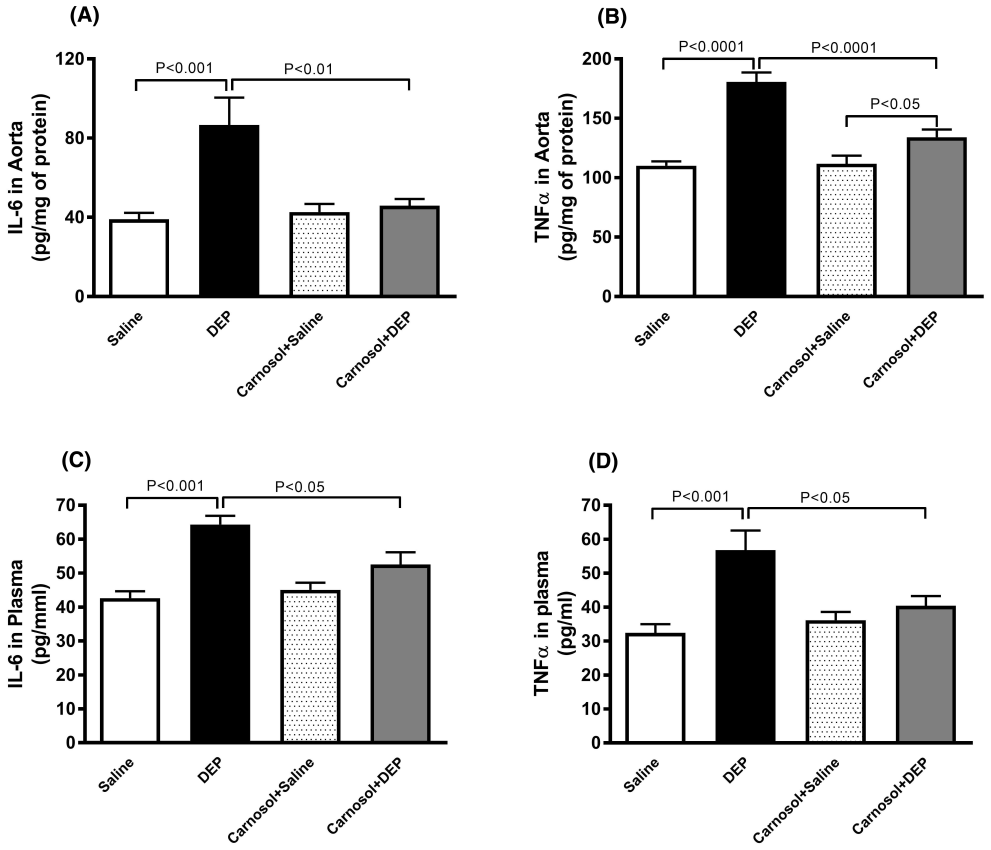

FIGURE 6 Interleukin-6 (IL-6; A and C) and tumor necrosis factor α (TNFα; B and D) concentrations in aortic tissue homogenates and plasma, 24 h after pulmonary administration of either saline or diesel exhaust particles (DEP; 20 μg/mouse) with or without carnosol pretreatment (20 mg/kg) given 1 h earlier. Data are means ± SEM ($n = 7–8$). Statistical analysis was by Holm–Sidak's multiple comparisons test.

the consequences of the expressions of vascular adhesion molecules, we evaluated the impact of DEP on vascular inflammation, oxidative damage, and DNA injury. It is well recognized that inflammation and oxidative stress are interrelated and that they mutually initiate and amplify each other.[2,42] Our data show that DEP induced a substantial increase in the concentrations of the pro-inflammatory cytokines IL-6 and TNFα in the plasma and aortic tissue homogenates. Likewise, following the exposure to DEP, we observed a significant increase in the concentration of TBARS on one hand, and on the other hand the activity of SOD and the concentration of GSH in the aortic tissue homogenates. The decrease in antioxidants SOD and GSH suggests the depletion of antioxidant protections.[43,44] Remarkably, the treatment with carnosol has significantly averted both the vascular inflammation and oxidative damage triggered by DEP. In line with our findings, it has been demonstrated that carnosol attenuated bleomycin-induced lung damage in rats and renal injury induced by unilateral ureteral obstruction in mice by suppressing oxidative damage and inflammation.[9,15] Evidence from experimental and clinical studies have demonstrated that exposure to particulate air pollution promotes a prooxidant and proinflammation situations which are associated with oxidative damage to DNA in various organs and circulating blood cells.[45] We have previously reported that exposure to DEP induce cardiac inflammation, oxidative damage, and DNA injury and that the treatment with nootkatone, a sesquiterpenoid found in grapefruit, prevented these actions.[18] Here, we found that carnosol treatment potently averted DEP-induced DNA injury in the vasculature. A recent study has reported that carnosol averts ultraviolet B-light-induced non-melanoma skin cancer formation through its inhibition of oxidative damage and ensuing DNA injury.[46]

In order to further assess the mechanism by which carnosol is exerting its protective mechanisms in the vasculature, we quantified the expression of Nrf2 and HO-1 concentrations in aortic homogenates of mice. Nrf2 is a central transcription factor which exerts a key cytoprotective action by regulating the expression of genes coding for antioxidant, anti-inflammatory and detoxifying proteins.[47] Under oxidative stress condition, the oxidant promote the breakdown of the Nrf2-Keap1-Cullin3 complex, allowing Nrf2 to heterodimerize with Jun and sMaf proteins.[47] Nrf2 will then translocate from the cytoplasm into the nucleus where it binds to the antioxidant response element, a regulatory enhancer region within gene promoters.[47] Consequently, the activated Nrf2 regulates the proteins with antioxidant activities, including HO-1, catalase, SOD and glutathione peroxidase 1.[47] Using the angiotensin II-induced vascular injury model in mice, it has been demonstrated that exposure to particulate matter is associated with vascular wall thickening and that Nrf2 knockout mice exhibited an aggravation of this action,

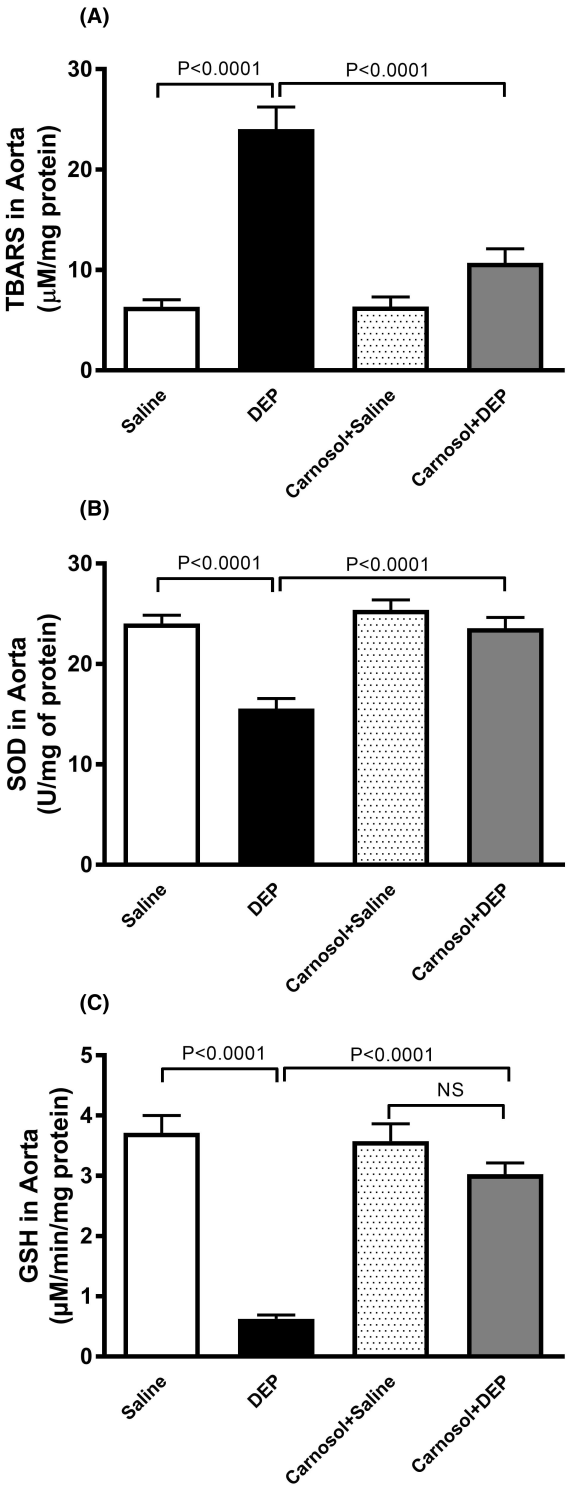

FIGURE 7 Thiobarbituric acid reactive substances (TBARS) concentration (A), superoxide dismutase (SOD) activity (B) and glutathione (GSH) concentration (C) in aortic tissue homogenates, 24 h after pulmonary administration of either saline or diesel exhaust particles (DEP; 20 μg/mouse) with or without carnosol pretreatment (20 mg/kg) given 1 h earlier. Data are means ± SEM ($n = 8$). Statistical analysis was by Holm–Sidak's multiple comparisons test.

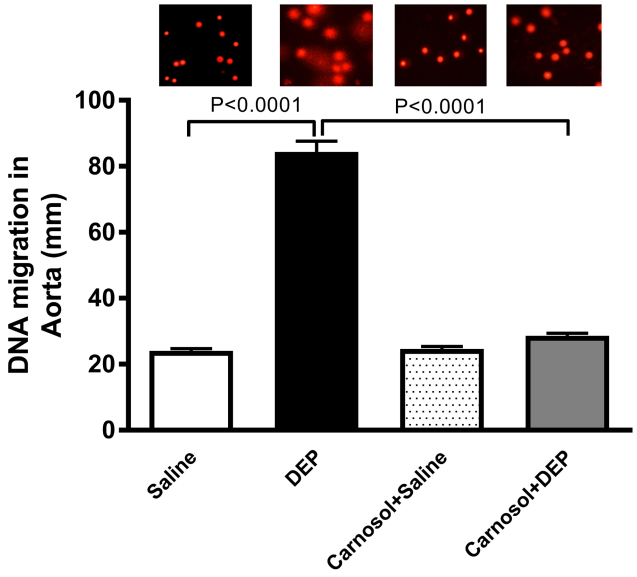

FIGURE 8 DNA migration (mm) in the aortic tissue evaluated by Comet assay, 24 h after pulmonary administration of either saline or diesel exhaust particles (DEP; 20 μg/mouse) with or without carnosol pretreatment (20 mg/kg) given 1 h earlier. Data are means ± SEM ($n = 5$). Statistical analysis was by Holm–Sidak's multiple comparisons test.

illustrating the important protective role played by Nrf2.[48] Our data show that carnosol restored the levels of both Nrf2 and HO-1 which were substantially decreased by DEP exposure in the aortic tissue. These results are in complete agreement with the action of carnosol in the re-establishment of the activity of SOD and concentration of GSH which were depleted by DEP administration. Also, our data corroborate previous findings which reported that carnosol protects against spinal cord injury-induced inflammation and oxidative damage by activating Nrf-2 in rats.[48]

In the present study, besides the use of carnosol for the first time in the context of protection against the pulmonary exposure of particulate air pollution-induced thrombogenicity, we have explored the possible alleviating effects of this compound on DEP-induced aortic inflammation, oxidative damage, and DNA injury which we did not report before. In our previous studies, we assessed the possible mitigating effects of other phytochemical compounds including emodin, nootkatone, thymoquinone on thrombogenicity, and heart tissue injury.[18,49,50] All the aforementioned compounds have offered protective effects.[18,49,50] However, additional work is required to assess whether carnosol is more effective than the above-mentioned phytochemical compounds and whether carnosol may offer protection against other pollutants.

The present study has some limitations. Presently, carnosol was given intraperitoneally, and hence can reach various organs including the lung. However, we are not able to specify whether

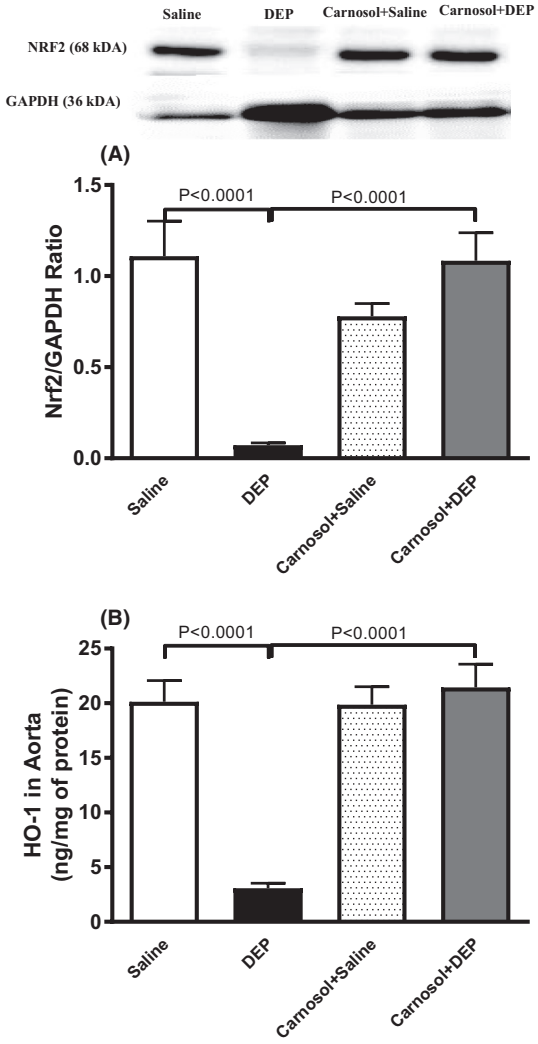

FIGURE 9 Expression of nuclear factor erythroid 2-related factor 2 (Nrf2; A) assessed by Western blotting and heme oxygenase-1 (HO-1; B) concentrations quantified by ELISA in aortic tissue homogenates, 24 h after pulmonary administration of either saline or diesel exhaust particles (DEP; 20 μg/mouse) with or without carnosol pretreatment (20 mg/kg) given 1 h earlier. Data are means ± SEM ($n = 8$). Statistical analysis was by Holm–Sidak's multiple comparisons test.

carnosol is exerting its protective on the lung (site of deposition of DEP) or on the vasculature or both. Further work is needed to address this issue. The dose of DEP used here is similar to those used in experimental animal models to study the pathophysiologic effects of particulate air pollution and has been shown to be representative to human exposure scenarios encountered during short-term extreme air pollution episodes to particulate matter ≤10 μm (PM_{10}).[51–54] However, one must consider that, in comparison with PM_{10}, DEP comprise a substantial amount of ultrafine particles. Therefore, we consider the current dosage to be high, particularly concerning human daily exposure to particulate air pollution in large urban areas.

In conclusion, our study provides compelling evidence that carnosol administration effectively mitigated DEP-induced thrombotic events, both in vivo and in vitro, as well as vascular inflammation, oxidative damage, and DNA injury by upregulating Nrf2 and HO-1. Subject to additional pharmacological and toxicological investigations, carnosol could be deemed a valuable agent with the potential to mitigate or protect against the vascular damage observed in individuals residing in urban areas with elevated levels of particulate air pollution.

AUTHOR CONTRIBUTIONS

SB, NEZ, and OE: Investigation; methodology; data curation; formal analysis. AA, AA, KA, and NA: Investigation; Methodology. AN: Conceptualization; formal analysis; funding acquisition; supervision; writing—review and editing; project administration; resources.

ACKNOWLEDGMENTS

This work was funded by grants from the UAE University, the College of Medicine and Health Sciences, the Zayed Center for Health Sciences, and the Summer Undergraduate Research Experience (SURE).

FUNDING INFORMATION

This work was supported by the UAEU, CMHS grant, Zayed Center for Health Sciences grant and Summer Undergraduate Research Experience (SURE) grant.

CONFLICT OF INTEREST STATEMENT

The authors report no conflicts of interest.

DATA AVAILABILITY STATEMENT

The data that support the findings of this study are available from the corresponding author upon reasonable request.

ETHICS STATEMENT

This research project received approval from the United Arab Emirates University (UAEU) Animal Ethics Committee (approval number: ERA_2021_8443), and all experiments adhered to protocols approved by the UAEU Animal Care and Research Advisory Committee.

ORCID

Abdulrahman Alkaabi https://orcid.org/0009-0004-7051-6448
Abderrahim Nemmar https://orcid.org/0000-0002-0699-1015

REFERENCES

1. Cohen AJ, Brauer M, Burnett R, et al. Estimates and 25-year trends of the global burden of disease attributable to ambient air pollution: an analysis of data from the Global Burden of Diseases Study 2015. *Lancet*. 2017;389:1907-1918.
2. Miller MR, Newby DE. Air pollution and cardiovascular disease: car sick. *Cardiovasc Res*. 2020;116:279-294. doi:10.1093/cvr/cvz228
3. Joshi SS, Miller MR, Newby DE. Air pollution and cardiovascular disease: the Paul Wood Lecture, British Cardiovascular Society 2021. *Heart*. 2022;108:1267-1273. doi:10.1136/heartjnl-2021-319844

4. Nemmar A, Holme JA, Rosas I, Schwarze PE, Alfaro-Moreno E. Recent advances in particulate matter and nanoparticle toxicology: a review of the in vivo and in vitro studies. *Biomed Res Int*. 2013;2013:279371.
5. Fathieh S, Grieve SM, Negishi K, Figtree GA. Potential biological mediators of myocardial and vascular complications of air pollution—a state-of-the-art review. *Heart Lung Circ*. 2022;32:26-42. doi:10.1016/j.hlc.2022.11.014
6. Kashyap D, Kumar G, Sharma A, Sak K, Tuli HS, Mukherjee TK. Mechanistic insight into carnosol-mediated pharmacological effects: recent trends and advancements. *Life Sci*. 2017;169:27-36. doi:10.1016/j.lfs.2016.11.013
7. Gonçalves C, Fernandes D, Silva I, Mateus V. Potential anti-inflammatory effect of *Rosmarinus officinalis* in preclinical in vivo models of inflammation. *Molecules*. 2022;27:609. doi:10.3390/molecules27030609
8. Alsamri H, El Hasasna H, Al Dhaheri Y, Eid AH, Attoub S, Iratni R. Carnosol, a natural polyphenol, inhibits migration, metastasis, and tumor growth of breast cancer via a ROS-dependent proteasome degradation of STAT3. *Front Oncol*. 2019;9:743. doi:10.3389/fonc.2019.00743
9. Kalantar H, Sadeghi E, Abolnezhadian F, et al. Carnosol attenuates bleomycin-induced lung damage via suppressing fibrosis, oxidative stress and inflammation in rats. *Life Sci*. 2021;287:120059. doi:10.1016/j.lfs.2021.120059
10. Nemmar A, Al Maskari S, Ali BH, Al Amri IS. Cardiovascular and lung inflammatory effects induced by systemically administered diesel exhaust particles in rats. *Am J Physiol Lung Cell Mol Physiol*. 2007;292:L664-L670.
11. Singh P, DeMarini D, Dick C, et al. Sample characterization of automobile and forklift diesel exhaust particles and comparative pulmonary toxicity in mice. *Environ Health Perspect*. 2004;112:820-825. doi:10.1289/ehp.6579
12. Morimoto Y, Izumi H, Yoshiura Y, et al. Comparison of pulmonary inflammatory responses following intratracheal instillation and inhalation of nanoparticles. *Nanotoxicology*. 2016;10:607-618.
13. Driscoll KE, Costa DL, Hatch G, et al. Intratracheal instillation as an exposure technique for the evaluation of respiratory tract toxicity: uses and limitations. *Toxicol Sci*. 2000;55:24-35.
14. Rahnama M, Mahmoudi M, Zamani Taghizadeh Rabe S, et al. Evaluation of anti-cancer and immunomodulatory effects of carnosol in a Balb/c WEHI-164 fibrosarcoma model. *J Immunotoxicol*. 2015;12:231-238. doi:10.3109/1547691x.2014.934975
15. Park JH, Leem J, Lee SJ. Protective effects of carnosol on renal interstitial fibrosis in a murine model of unilateral ureteral obstruction. *Antioxidants (Basel)*. 2022;11:2341. doi:10.3390/antiox11122341
16. Nemmar A, Al-Salam S, Yuvaraju P, Beegam S, Yasin J, Ali BH. Chronic exposure to water-pipe smoke induces cardiovascular dysfunction in mice. *Am J Physiol Heart Circ Physiol*. 2017;312:H329-H339.
17. Nemmar A, Yuvaraju P, Beegam S, John A, Raza H, Ali BH. Cardiovascular effects of nose-only water-pipe smoking exposure in mice. *Am J Physiol Heart Circ Physiol*. 2013;305:H740-H746.
18. Nemmar A, Al-Salam S, Beegam S, Yuvaraju P, Ali BH. Thrombosis, systemic and cardiac oxidative stress and DNA damage induced by pulmonary exposure to diesel exhaust particles, and the effect of nootkatone thereon. *Am J Physiol Heart Circ Physiol*. 2018;314:H917-H927. doi:10.1152/ajpheart.00313.2017
19. Nemmar A, Beegam S, Zaaba NE, Alblooshi S, Alseiari S, Ali BH. The salutary effects of Catalpol on diesel exhaust particles-induced thrombogenic changes and cardiac oxidative stress, inflammation and apoptosis. *Biomedicine*. 2022;10:99. doi:10.3390/biomedicines10010099
20. Ferdous Z, Beegam S, Zaaba NE, et al. Exacerbation of thrombotic responses to silver nanoparticles in hypertensive mouse model. *Oxidative Med Cell Longev*. 2022;2022:2079630. doi:10.1155/2022/2079630
21. Nemmar A, Al-Salam S, Beegam S, Yuvaraju P, Ali BH. Aortic oxidative stress, inflammation and DNA damage following pulmonary exposure to cerium oxide nanoparticles in a rat model of vascular injury. *Biomolecules*. 2019;9:376. doi:10.3390/biom9080376
22. Dasgupta A, Klein K. *Antioxidants in Food, Vitamins and Supplements*. Prevention and Treatment of Disease; 2014.
23. Aguilar Diaz De Leon J, Borges CR. Evaluation of oxidative stress in biological samples using the thiobarbituric acid reactive substances assay. *J Vis Exp*. 2020;2020:e61122. doi:10.3791/61122
24. Devasagayam TP, Boloor KK, Ramasarma T. Methods for estimating lipid peroxidation: an analysis of merits and demerits. *Indian J Biochem Biophys*. 2003;40:300-308.
25. Bhagwat SV, Vijayasarathy C, Raza H, Mullick J, Avadhani NG. Preferential effects of nicotine and 4-(N-methyl-N-nitrosamine)-1-(3-pyridyl)-1-butanone on mitochondrial glutathione S-transferase A4-4 induction and increased oxidative stress in the rat brain. *Biochem Pharmacol*. 1998;56:831-839.
26. John A, Raza H. Alterations in inflammatory cytokines and redox homeostasis in LPS-induced pancreatic Beta-cell toxicity and mitochondrial stress: protection by Azadirachtin. *Front Cell Dev Biol*. 2022;10:867608. doi:10.3389/fcell.2022.867608
27. Hartmann A, Speit G. The contribution of cytotoxicity to DNA-effects in the single cell gel test (comet assay). *Toxicol Lett*. 1997;90:183-188.
28. Nemmar A, Al-Salam S, Yuvaraju P, Beegam S, Yasin J, Ali BH. Chronic exposure to water-pipe smoke induces alveolar enlargement, DNA damage and impairment of lung function. *Cell Physiol Biochem*. 2016;38:982-992.
29. Nemmar A, Karaca T, Beegam S, Yuvaraju P, Yasin J, Ali BH. Lung oxidative stress, DNA damage, apoptosis, and fibrosis in adenine-induced chronic kidney disease in mice. *Front Physiol*. 2017;8:896.
30. Collaborators GBD, Ärnlöv J. Global burden of 87 risk factors in 204 countries and territories, 1990–2019: a systematic analysis for the Global Burden of Disease Study 2019. *Lancet*. 2020;396:1223-1249.
31. Al-Kindi SG, Brook RD, Biswal S, Rajagopalan S. Environmental determinants of cardiovascular disease: lessons learned from air pollution. *Nat Rev Cardiol*. 2020;17:656-672. doi:10.1038/s41569-020-0371-2
32. Liu Y, Pan J, Fan C, et al. Short-term exposure to ambient air pollution and mortality from myocardial infarction. *J Am Coll Cardiol*. 2021;77:271-281. doi:10.1016/j.jacc.2020.11.033
33. Morimoto Y, Izumi H, Yoshiura Y, et al. Basic study of intratracheal instillation study of nanomaterials for the estimation of the hazards of nanomaterials. *Ind Health*. 2018;56:30-39. doi:10.2486/indhealth.2017-0082
34. Turner PV, Brabb T, Pekow C, Vasbinder MA. Administration of substances to laboratory animals: routes of administration and factors to consider. *J Am Assoc Lab Anim Sci*. 2011;50:600-613.
35. Lee J-J, Jin Y-R, Lim Y, et al. Antiplatelet activity of carnosol is mediated by the inhibition of TXA2 receptor and cytosolic calcium mobilization. *Vasc Pharmacol*. 2006;45:148-153. doi:10.1016/j.vph.2006.04.003
36. Baccarelli A, Zanobetti A, Martinelli I, et al. Effects of exposure to air pollution on blood coagulation. *J Thromb Haemost*. 2007;5:252-260.
37. Franchini M, Mengoli C, Cruciani M, Bonfanti C, Mannucci PM. Association between particulate air pollution and venous thromboembolism: a systematic literature review. *Eur J Intern Med*. 2016;27:10-13.
38. Hantrakool S, Kumfu S, Chattipakorn SC, Chattipakorn N. Effects of particulate matter on inflammation and thrombosis: past evidence for future prevention. *Int J Environ Res Public Health*. 2022;19:8771. doi:10.3390/ijerph19148771
39. Costa A, Pasquinelli G. Air pollution exposure induces vascular injury and hampers endothelial repair by altering progenitor and stem cells functionality. *Front Cell Dev Biol*. 2022;10:897831.

40. Lian KC, Chuang JJ, Hsieh CW, et al. Dual mechanisms of NF-kappaB inhibition in carnosol-treated endothelial cells. *Toxicol Appl Pharmacol*. 2010;245:21-35. doi:10.1016/j.taap.2010.01.003
41. Yao H, Chen Y, Zhang L, et al. Carnosol inhibits cell adhesion molecules and chemokine expression by tumor necrosis factor-α in human umbilical vein endothelial cells through the nuclear factor-κB and mitogen-activated protein kinase pathways. *Mol Med Rep*. 2014;9:476-480. doi:10.3892/mmr.2013.1839
42. Lawal AO, Davids LM, Marnewick JL. Diesel exhaust particles and endothelial cells dysfunction: an update. *Toxicol In Vitro*. 2016;32:92-104. doi:10.1016/j.tiv.2015.12.015
43. Scandalios JG. Oxidative stress: molecular perception and transduction of signals triggering antioxidant gene defenses. *Braz J Med Biol Res*. 2005;38:995-1014.
44. Nemmar A, Yuvaraju P, Beegam S, Fahim MA, Ali BH. Cerium oxide nanoparticles in lung acutely induce oxidative stress, inflammation, and DNA damage in various organs of mice. *Oxidative Med Cell Longev*. 2017;2017:9639035.
45. Moller P, Danielsen PH, Karottki DG, et al. Oxidative stress and inflammation generated DNA damage by exposure to air pollution particles. *Mutat Res Rev Mutat Res*. 2014;762:133-166.
46. Tong L, Wu S. The mechanisms of Carnosol in chemoprevention of ultraviolet B-light-induced non-melanoma skin cancer formation. *Sci Rep*. 2018;8:3574. doi:10.1038/s41598-018-22029-x
47. Abdelrahman AM, Al Suleimani Y, Shalaby A, et al. Effect of canagliflozin, a sodium glucose co-transporter 2 inhibitor, on cisplatin-induced nephrotoxicity in mice. *Naunyn Schmiedebergs Arch Pharmacol*. 2019;392:45-53. doi:10.1007/s00210-018-1564-7
48. Gao M, Ma Y, Luo J, et al. The role of Nrf2 in the PM-induced vascular injury under real ambient particulate matter exposure in C57/B6 mice. *Front Pharmacol*. 2021;12:618023. doi:10.3389/fphar.2021.618023
49. Nemmar A, Al DR, Alamiri J, et al. Diesel exhaust particles induce impairment of vascular and cardiac homeostasis in mice: ameliorative effect of Emodin. *Cell Physiol Biochem*. 2015;36:1517-1526.
50. Nemmar A, Al-Salam S, Zia S, et al. Contrasting actions of diesel exhaust particles on the pulmonary and cardiovascular systems and the effects of thymoquinone. *Br J Pharmacol*. 2011;164:1871-1882.
51. Nemmar A, Hoet PH, Dinsdale D, Vermylen J, Hoylaerts MF, Nemery B. Diesel exhaust particles in lung acutely enhance experimental peripheral thrombosis. *Circulation*. 2003;107:1202-1208.
52. Mutlu GM, Green D, Bellmeyer A, et al. Ambient particulate matter accelerates coagulation via an IL-6-dependent pathway. *J Clin Invest*. 2007;117:2952-2961.
53. Richman BT. Air pollution in the world's megacities. *Environment*. 1994;36:2-13, 25-37.
54. Marlier ME, Jina AS, Kinney PL, DeFries RS. Extreme air pollution in global megacities. *Curr Clim Chang Rep*. 2016;2:15-27. doi:10.1007/s40641-016-0032-z

SUPPORTING INFORMATION

Additional supporting information can be found online in the Supporting Information section at the end of this article.

How to cite this article: Beegam S, Zaaba NE, Elzaki O, et al. Palliative effects of carnosol on lung-deposited pollutant particles-induced thrombogenicity and vascular injury in mice. *Pharmacol Res Perspect*. 2024;12:e1201. doi:10.1002/prp2.1201